AN ACCURATE MASS OF THE 31 CYGNI RED SUPERGIANT

Philip D. Bennett (Dalhousie University)

Alexander Brown & Thomas Ayres (CASA, University of Colorado)

1. Introduction

Red supergiants (RSGs) are massive, evolved stars that are among the brightest stars in the near infrared. But the uncertain physics of mass loss limits the ability of evolutionary models to accurately represent these stars in detail. Lacking a fundamental, predictive theory of mass loss, this process is normally incorporated into stellar models using simple parametric formulas such as Reimer's Law. In this situation, it is important to constrain theoretical models evolved using such mass loss parametrizations by observational determination of fundamental parameters. But observational constraints make RSG binaries difficult targets – their orbital periods are long (often decades), and the brightness of the supergiant primaries overwhelm the light of their main sequence companions in the optical and near infrared. The first difficulty (long period) simply requires patience, the second (composite spectrum) is best handled by looking where the main sequence companion is brighter – in the ultraviolet (UV) spectrum.

The best region of the UV for this purpose is the far UV (FUV) shortward of 1400 Å, where numerous strong lines provide suitable benchmarks for velocity cross-correlation of spectra, but this requires access to a space-based observatory. Currently the only telescope with appropriate FUV spectroscopic capability is the ***Hubble Space Telescope***. In particular, the *HST* ***Space Telescope Imaging Spectrograph (STIS)*** high-resolution echelle modes are ideal for this task. Here, we present the results of ***HST/STIS*** observations of the bright, eclipsing K supergiant binary system 31 Cygni (K4 Ib + B3 V), with the goal of determining accurate masses of the 31 Cygni stars. See Figure 1 below, and Figure 2 at right.

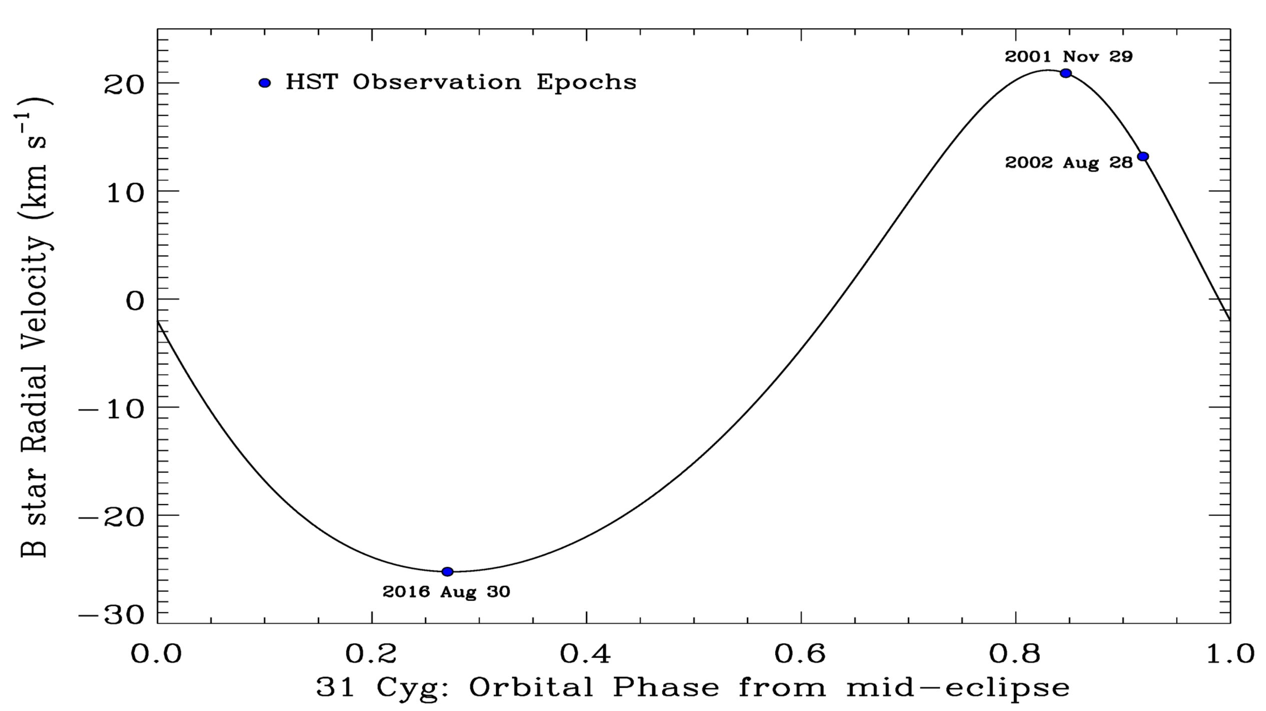

Figure 1. The predicted radial velocity curve for the 31 Cyg B-type secondary, from Griffin (2008) and Eaton (2003).

2. Reduction & Analysis

The HST/STIS echelle modes return a 2-dimensional image with the order stacked (cross-dispersed) perpendicular to the dispersion direction. These must be extracted and reduced to produce a 1-dimensional spectrum for analysis. Briefly, for the 31 Cyg STIS observations presented here, each echellogram was order-merged, an "active" blaze correction applied, new wavelength dispersion relations calculated, and post-facto correction for higher-order wavelength errors applied. Then, spectra from different echelle settings were spliced together, adjusting the relative flux levels if necessary based on the apparent intensities in any overlapping regions, and adjusting the relative wavelengths using cross-correlation of features in the overlap regions. Each spectral window of the three observation epochs (2, 3 and 4; see Table 1) was correlated with the corresponding window of the other epochs, so a total of 6 correlations (for each of the 6 windows) were obtained for each of the 3 possible epoch cross-correlations: epochs 2-3, 2-4 and 3-4. The 18 wavelength shifts obtained were converted to radial velocity differences. The results are shown in Table 2. For binary orbital motion, from Equation (5), these differences should be proportional to the differences in the expression $\cos(v_i + \omega)$ at observation epochs i and j.

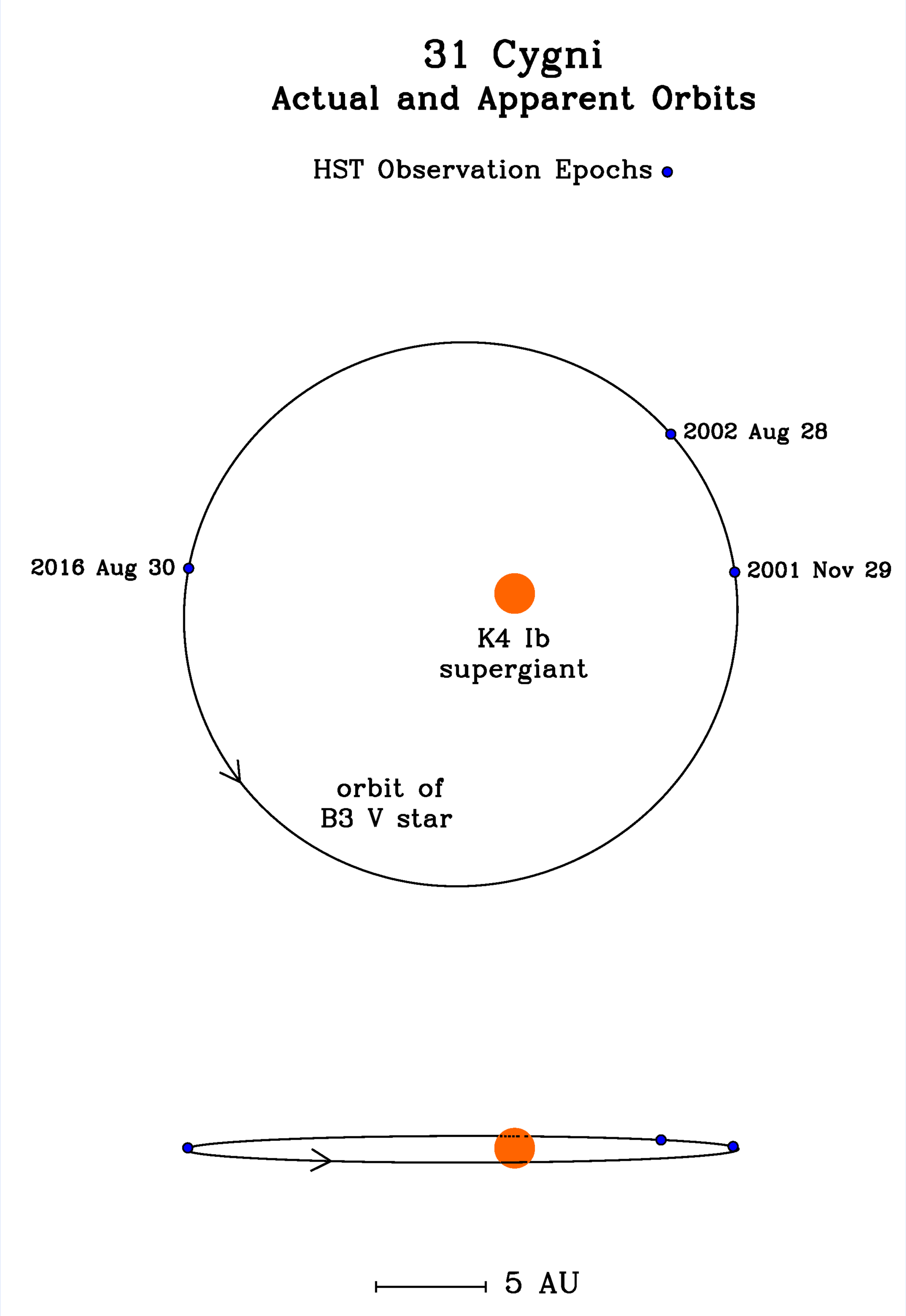

Figure 2. The orbit of 31 Cygni drawn to scale, with orbital configurations at HST observation epochs shown.

3. Observations

Observations of the FUV spectrum of 31 Cyg with the *HST/STIS* E140H high-resolution echelle modes were obtained at 3 epochs over the period 2001—2016, spanning about 1.5 orbits of 31 Cyg. The date, orbital phase, and true anomaly of these observations are shown in Table 1, and positions shown on Figure 2 above. The first observation (Epoch 1) failed to properly acquire the star in the STIS aperture, and was rescheduled as Epoch 2. The E140H wavelength range was from 1150 – 1440 A. Predicted radial velocities are shown in Figure 1 at left. Varying orbital radial velocity is obvious in the spectra (Figure 3) below.

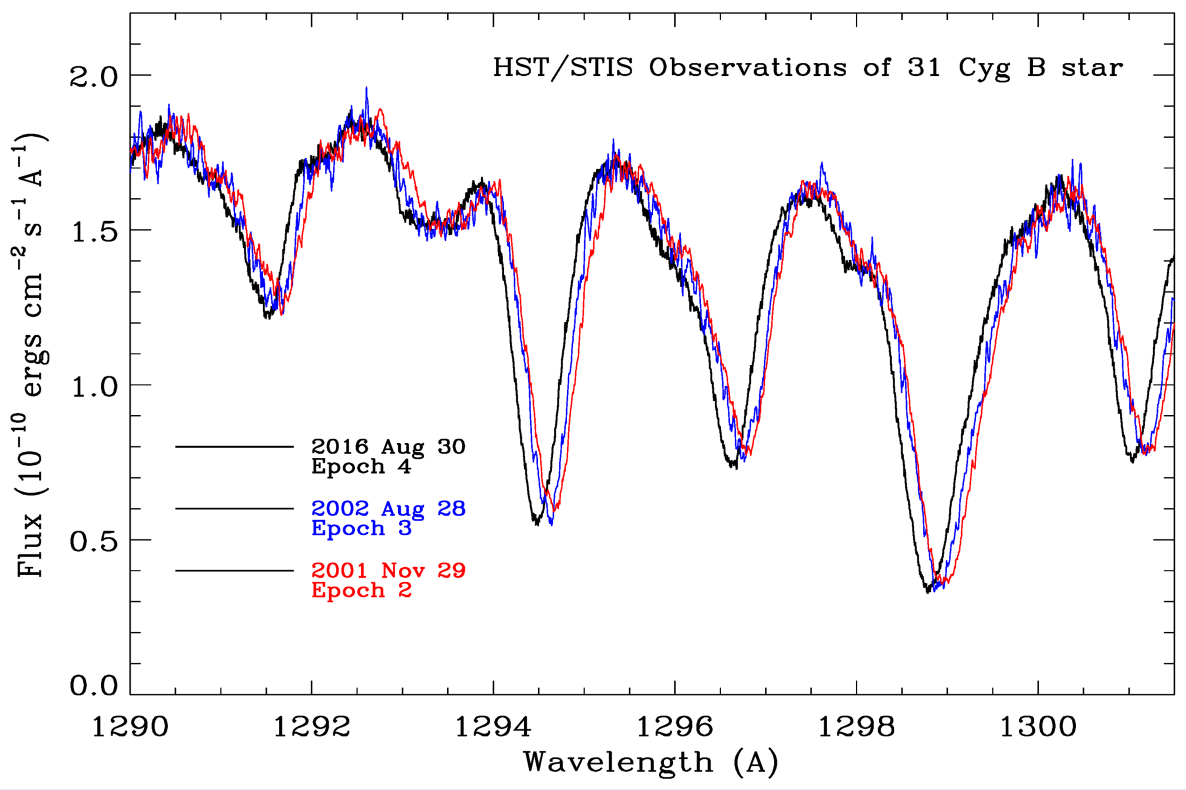

Figure 3. A comparison of the 1300 A region of the HST/STIS spectrum at the 3 observation epochs. The wavelength shifts due to orbital radial velocity are obvious.

4. Determination of the Binary Orbit

The 31 Cygni binary has an orbital period of $P = 3784.3$ days (= 10.36 yrs). In the optical, the red supergiant dominates the spectrum. Even assuming the secondary spectrum can be successfully disentangled, the companion's spectrum is that of an early B-type main-sequence star: a mostly featureless continuum dominated by the Stark-broadened Balmer lines of hydrogen. This is a spectrum that is poorly suited for radial velocity work. Wright's (1970) value of the secondary's radial velocity (RV) semi-amplitude, $K_2 = 20.8 \pm 3.8$ km s^{-1}, is about the best possible from a ground-based site. Eaton (2003) obtained $K_2 = 23.2 \pm 1.0$ km s^{-1} using UV spectroscopy from the ***International Ultraviolet Explorer*** (***IUE***) satellite.

Both stellar orbits in a binary system have identical elements, except for their semimajor axes a_1, a_2, defined from the binary's center of mass. The semimajor axis of the relative orbit is then given by $a = a_1 + a_2$, and we also have the relation $M_1 a_1 = M_2 a_2$ from the definition of center of mass. The only independent orbital element of the companion's orbit is the semi-major axis a_2. The spectroscopic observable is actually the radial velocity semi-amplitude, K_2, defined in terms of the orbital elements as

$$K_2 = \frac{2\pi a_2 \sin i}{P\sqrt{1 - e^2}}\,, \qquad (1)$$

where $e = 0.2084 \pm 0.0031$ is the orbital eccentricity (Griffin 2008), and the orbital inclination $i \approx 90°$, $\sin i \simeq 1$ because the system must be seen nearly edge-on for eclipses to occur. Then,

$$\frac{K_2}{K_1} = \frac{a_2}{a_1} = \frac{M_1}{M_2} \qquad (2)$$

and so the ratio of the RV semi-major amplitudes determines the ratio of the stellar masses. And from Kepler's 3rd Law,

$$M_1 + M_2 = \frac{4\pi^2 a^3}{G P^2} \qquad (3)$$

where G is the gravitational constant. If the ratio K_2/K_1 is known, then both masses are determined. For 31 Cygni, the orbit of K supergiant primary star is well determined with $K_1 = 13.94 \pm 0.04$ km s^{-1} (Griffin 2008). Therefore, all we need to determine the stellar masses is an accurate value of K_2. To do this well, we need to observe the FUV spectrum of 31 Cyg, where the spectrum has a number of strong lines appropriate for RV analysis. The radial velocity V of the secondary star is given by (cf., Green 1985).

$$V = V_0 + K_2[\cos(v + \omega) + e\cos\omega] \qquad (4)$$

where V_0 is the systemic velocity of the center of mass (barycenter) of the binary, v is the true anomaly, and ω is the argument of periastron. Then, the radial velocity difference $\Delta V_{ij} = V_i - V_j$ between two radial observations at epochs i and
and j is just

$$\Delta V_{ij} = K_2\left[\cos(v_i + \omega) - \cos(v_j + \omega)\right] \qquad (5)$$

In order to determine K_2, all that is minimally needed are the RV differences between two sets of observations. With the three sets of FUV observations available for 31 Cyg, we have redundancy that allows for an assessment of the measurement error.

Table 1. ***HST/STIS*** **observation epochs of 31 Cygni.**

Epoch	Date	Orbital Phase φ [from mid-eclipse]	True Anomaly v (deg) [from periastron]
2	2001 Nov 29	0.84659	344.842
3	2002 Aug 28	0.91846	24.895
4	2016 Aug 30	0.27035	154.666

Table 2: Cross-correlation analysis of E140H spectra of 31 Cygni. Velocities ΔV_{ij} are in km s^{-1}.

Region	Wavelengths (A)	ΔV_{32}	ΔV_{43}	ΔV_{42}	ΔV_{234}	$C_{32}^{\max}$	$C_{43}^{\max}$	$C_{42}^{\max}$
A	1222.5 – 1250	10.81	26.12	37.56	-0.63	0.868	0.863	0.941
B	1338 – 1365	9.87	28.62	37.08	+1.41	0.717	0.760	0.841
C	1365 – 1392	9.44	30.92	39.25	+1.11	0.613	0.695	0.789
E	1157 – 1192.5	11.39	29.51	39.40	+1.50	0.786	0.806	0.913
F1	1267 – 1283.25	8.66	28.20	37.60	-0.74	0.906	0.916	0.959
F2	1283.25 – 1300.35	10.78	24.41	35.58	-0.29	0.970	0.972	0.985

5. Results

In Table 2, each ΔV_{ij} is the RV difference between observation epochs i and and j. The ΔV_{234} values,

$$\Delta V_{234} = V_{32} + \Delta V_{43} - \Delta V_{42} = 0$$

are the cyclic checksum of RV differences from epochs 2 ⟶ 3 ⟶ 4 ⟶ 2 and should be identically equal to zero. The actual (nonzero) value of ΔV_{234} therefore provides a check of the accuracy of the inferred radial velocity differences ΔV_{ij}. The $C_{ij}^{\max}$ values are the maximums of the cross-correlation curve of the spectrum at epoch i and the spectrum at epoch j. For two identical spectra with zero noise, this value would be exactly 1. For two spectra with relative flux errors σ, the cross-correlation maximum would be $\sim 1 - 1/\sigma^2$, and so $1 - C_{ij}^{\max}$ provides an estimate of $1/\sigma^2$.

The radial velocity differences ΔV_{ij} should be proportional to the expression

$$\cos(v_i + \omega) - \cos(v_j + \omega)$$

appearing on the right-hand side of Equation (5), with the constant of proportionality being the desired secondary radial velocity semi-amplitude, K_2. The 18 values of ΔV_{32}, ΔV_{43}, and ΔV_{42} are plotted against the respective cosine argument; the result is shown in Figure 4 below.

A weighted linear least-squares fit to these 18 points by a line constrained to pass through the origin was carried out, yielding an estimate of the slope $K_2 =$ 18.0 km s^{-1} (Figure 4). Although the uncertainty in K_2 is ~1 km s^{-1}, the situation is complicated by the fact that the points in Figure 5 do not appear to lie on a straight line as expected. A possible explanation of this discrepancy is the presence of an unknown bias skewing the cross-correlation. Another possibility is that the Griffin (2008) solution of the primary orbit is not as accurate as believed. Further investigation is ongoing. In combination with Griffin's (2008) value of $K_1 = 13.94$ km s^{-1}, the value of $K_2 = 18.0$ km s^{-1} yields masses of $\boldsymbol{M_1 = 6.73\ M_\odot}$ and $\boldsymbol{M_2 = 5.22\ M_\odot}$ for the 31 Cyg stars.

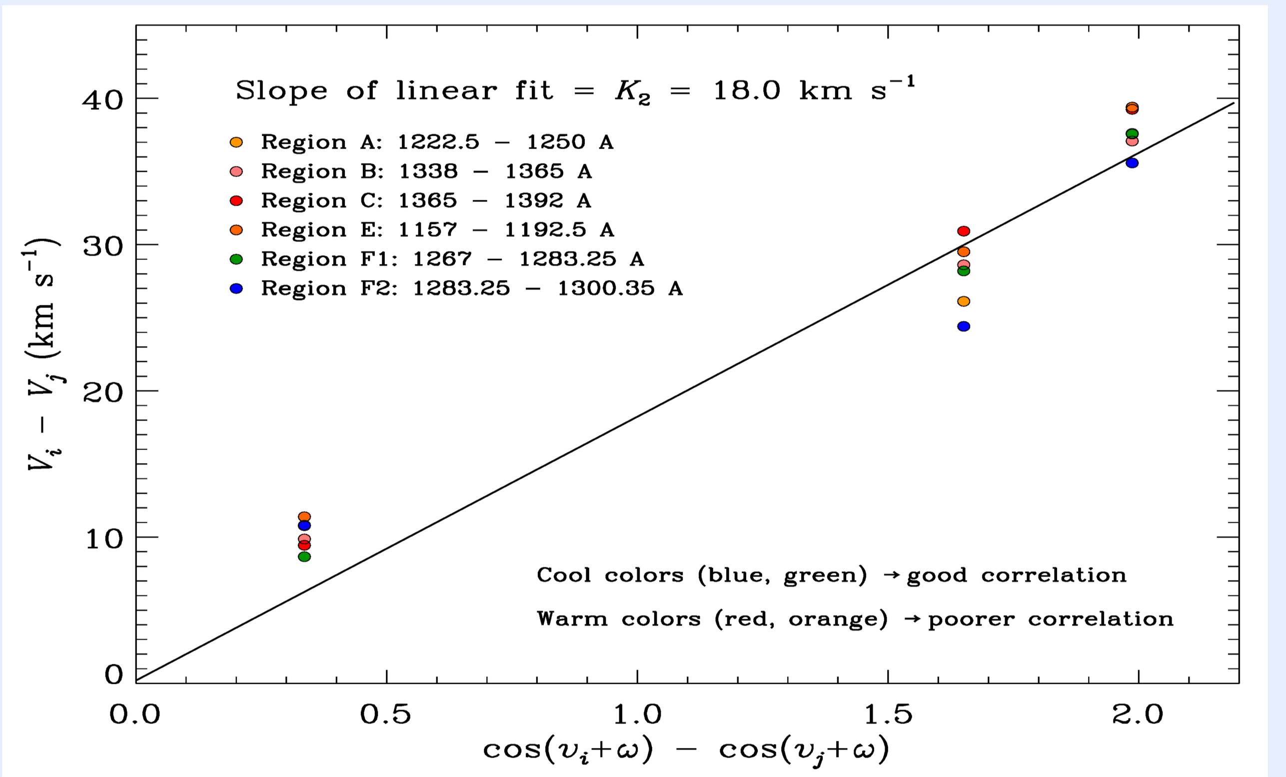

Figure 4. Determination of K_2 from radial velocity differences.

References

Eaton, J.A. 1993, AJ, 106, 2081

Green, R.M. 1985, *Spherical Astronomy*, Cambridge Univ. Press

Griffin, R.F. 2008, Observatory, 128, 362

Wright, K.O. 1970, Vistas in Astron., 12, 147